III

Publication III

Markku P. V. Stenberg and Tero T. Heikkilä, *Nonlinear shot noise in mesoscopic diffusive normal-superconducting systems*, Phys. Rev. B **66**, 144504 (2002).

http://link.aps.org/abstract/prb/v66/p144504

PHYSICAL REVIEW B **66**, 144504 (2002)

Nonlinear shot noise in mesoscopic diffusive normal-superconducting systems

Markku P. V. Stenberg and Tero T. Heikkilä
Materials Physics Laboratory, Helsinki University of Technology, P. O. Box 2200 (Technical Physics), FIN-02015 HUT, Finland
(Received 27 February 2002; revised manuscript received 5 August 2002; published 16 October 2002)

We study differential shot noise in mesoscopic diffusive normal-superconducting (NS) heterostructures at finite voltages where nonlinear effects due to the superconducting proximity effect arise. A numerical scattering-matrix approach is adopted. Through an NS contact, we observe that the shot noise shows a reentrant dependence on voltage due to the superconducting proximity effect but the differential Fano factor stays approximately constant. Furthermore, we consider differential shot noise in the structures where an insulating barrier is formed between normal and superconducting regions and calculate the differential Fano factor as a function of barrier height.

DOI: 10.1103/PhysRevB.66.144504 PACS number(s): 74.40.+k,74.50.+r

Shot noise is fluctuation of the current that is due to the discrete nature of the charge carriers. It is the only source of noise at zero temperature. Current noise contains information on the physics of transport phenomenon not contained in the conductance. A classical value $S=2e|I|=S_{\rm Poisson}$ for the noise, observed, e.g., in a vacuum diode, is obtained in the tunneling limit, i.e., when the transmission probabilities for open scattering channels are small and there are no correlations among the charge carriers. However, two effects may reduce the noise below its Poissonian value: inelastic scattering (not considered in this paper) and reduced noise in channels with finite transmission amplitudes.[1] In a phase-coherent conductor, all the transfer coefficients are not necessarely small. Instead, e.g., in a diffusive phase-coherent metallic wire the distribution function of the transmission coefficients has a bimodal form[2] such that almost closed and almost open channels are preferred. This results in a shot noise that is one-third of the Poissonian noise independently of the sample-specific properties such as the number of channels or the degree of disorder.[1,3]

During the last decade the noise properties of mesoscopic conductors have been under intense study (for a review, see Ref. 4). There has also been increasing interest to comprehend the interplay of phase coherence and superconducting proximity effect in mesoscopic physics. Recently the doubling of the shot noise in normal-superconducting heterojunctions, predicted in the linear regime in Ref. 5, has been verified experimentally.[6] While the theory of classical shot noise and the quantum mechanical results in the linear regime have been discussed before, little attention has been paid to mesoscopic noise at finite voltages when the presence of superconductivity induces nonlinear behavior in the transport coefficients. In Ref. 7 current correlations in very small hybrid NS structures at finite voltages were discussed. Eliminating the effects due to the finite size of the structure and fully taking into account the effects arising in a diffusive phase-coherent sample, however, requires larger structures to be studied. In Ref. 8 a counting-field approach to the Keldysh Green's-function method was adopted to calculate numerically the statistics of current in a normal wire connected to normal and superconducting reservoirs at finite voltages. In this paper we use a well-established scattering-matrix approach to calculate the differential shot noise at finite voltages in the presence of the proximity effect.

We find that in the presence of superconductivity, the differential shot noise follows the reentrance peak observed in conductance such that the differential Fano factor remains approximately constant. In the NS structure the resulting differential Fano factor is twice its normal value. The Fano factor can be roughly interpreted to be the ratio of the effective charge-carrying unit and the unit charge. Hence the doubling of the shot noise is a signature of Cooper-pair transport in the NS junction.

In the second part of the paper, we consider differential shot noise in structures where an insulating tunneling barrier separates the normal and superconducting regions. In the tunneling limit differential conductance essentially probes the density of states in the superconducting side except that at zero voltage and low temperature the reflectionless-tunneling effect increases the differential conductance. Reflectionless tunneling arises because of the quantum coherence of electrons and Andreev-reflected holes that travel along the same paths in opposite directions scattering several times from the barrier and the disorder potential of the metal.[9–11] We calculate the differential shot noise as a function of voltage and predict that the reflectionless-tunneling effect is present not only in the differential conductance, but also in the differential shot noise, such that the differential Fano factor stays constant.

We consider the zero-frequency shot-noise power in a two-lead system that is the $\omega=0$ limit of the Fourier-transformed current-current correlation function

$$S=\int_{-\infty}^{\infty}dt\langle[\hat{I}(t)-\langle\hat{I}(t)\rangle][\hat{I}(0)-\langle\hat{I}(0)\rangle]\rangle, \tag{1}$$

where the current operator $\hat{I}(t)$ may be expressed through a scattering matrix $\mathbf{s}$ and $\langle\ \rangle$ denotes the quantum mechanical expectation value. In the NS junction where one reservoir is normal and the other is superconducting the two-terminal differential shot noise at zero temperature T takes the form[5]

$$\frac{1}{eG_0}\frac{dS}{dV}=2\,\mathrm{Tr}[\mathbf{s}_{11}^{ee}\mathbf{s}_{11}^{ee\dagger}(\mathbf{1}-\mathbf{s}_{11}^{ee}\mathbf{s}_{11}^{ee\dagger})+\mathbf{s}_{11}^{he}\mathbf{s}_{11}^{he\dagger}(\mathbf{1}-\mathbf{s}_{11}^{he}\mathbf{s}_{11}^{he\dagger}) +2\mathbf{s}_{11}^{ee}\mathbf{s}_{11}^{ee\dagger}\mathbf{s}_{11}^{he}\mathbf{s}_{11}^{he\dagger}]. \tag{2}$$

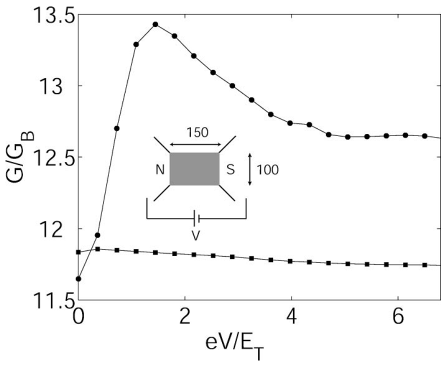

FIG. 1. Differential conductance as a function of voltage. Circles, NS structure depicted in the inset; squares, N structure. The 95% confidence interval for the relative error is $\pm 1\%$. The results in Figs. 1–3 were ensemble averaged over 600 realizations.

Here $\mathbf{s}_{11}^{he}$ ($\mathbf{s}_{11}^{ee}$) is the submatrix of the scattering matrix referring to the reflection as a hole (electron) of an electron incident in lead 1, evaluated at $E=eV$. At $T=0$ the differential conductance of the NS junction at voltage V is given by

$$G=G_0\,\mathrm{Tr}[\mathbf{s}_{21}^{ee}\mathbf{s}_{21}^{ee\dagger}+\mathbf{s}_{21}^{he}\mathbf{s}_{21}^{he\dagger}+2\mathbf{s}_{11}^{he}\mathbf{s}_{11}^{he\dagger}], \tag{3}$$

where the unit conductance of a single spin-degenerate channel is denoted by $G_0=2e^2/h$. In the absence of normal transmission for voltages below Δ/e Eq. (2) reduces to

$$\frac{1}{eG_0}\frac{dS}{dV}=8\,\mathrm{Tr}[\mathbf{s}_{11}^{he}\mathbf{s}_{11}^{he\dagger}(\mathbf{1}-\mathbf{s}_{11}^{he}\mathbf{s}_{11}^{he\dagger})] \tag{4}$$

and the conductance is directly proportional to the Andreev reflection probability,

$$G_{\mathrm{NS}}=2G_0\,\mathrm{Tr}[\mathbf{s}_{11}^{he}\mathbf{s}_{11}^{he\dagger}], \tag{5}$$

the factor of two indicating the fact that Andreev reflection creates a Cooper pair in the superconductor.

We have studied two kinds of NS heterostructures: a phase-coherent normal-metal wire connected from the one end to a normal-metal reservoir and from the other to a long superconductor, and an NIS structure including a tunneling barrier between the normal wire and the superconductor. In our calculations we adopt a scattering-matrix approach and apply a numerical decimation method to truncate the Green's function of the two-dimensional structure.[12] The disordered normal-metal structure is modeled by a tight-binding Hamiltonian with the site energies varying at random within range $[-\frac{1}{2}w,\frac{1}{2}w]$. Here we choose $w=\gamma$, where γ is the nearest-neighbor coupling parameter. The calculated values of the observables are averaged over several impurity configurations. The parameters of the structure are chosen such that the transport through the normal metal is diffusive, i.e., the mean free path l is much smaller than the length L of the structure, which on the other hand is much smaller than the localization length Nl, where N is the number of quantum channels ($l\ll L\ll Nl$). The length scales of the structures in units of the lattice constant are depicted in the insets of Figs. 1 and 4 illustrating the scattering geometries of the NS heterojunctions.

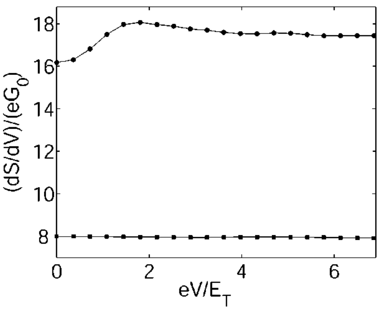

FIG. 2. Differential shot noise as a function of voltage. Circles, NS structure; squares, N structure. The 95% confidence interval for the relative error is $\pm 1\%$.

The influence of the proximity effect on current noise is most conveniently seen in the differential Fano factor $(dS/dV)/2eG$. In order to compare the electrical transport through normal and normal-superconducting structures we calculate $(dS/dV)/2eG$ in these two cases. The calculated differential conductances for normal (G_{N}) and NS (G_{NS}) structures are plotted as functions of voltage in Fig. 1. As expected, in NS conductance we observe the well-known nonlinear reentrant behavior due to the presence of the superconducting proximity effect, i.e, G_{NS} exhibits a maximum at energies of the order of a few Thouless energies $E_T=\hbar D/L^2$. At this energy scale G_{N} remains constant. At zero voltage, normal shot noise is known to have a value $S_{\mathrm{N}}=\frac{1}{3}S_{\mathrm{Poisson}}$. In the normal case there are no nonlinearities at this energy scale. Thus increasing voltage does not change this result and the differential shot noise dS_{N}/dV for the normal structure remains constant as shown in Fig. 2. In the NS case, however, the differential shot noise dS_{NS}/dV exhibits a similar reentrant effect as G_{NS}. This is in agreement with the counting-field approach of Ref. 8. Combining these two results, in the N structure, we observe that for the differential Fano factor the result $(dS_{\mathrm{N}}/dV)/2eG=1/3$ holds also for finite voltages, i.e., differential shot noise has the value one third of the Poisson value. In the NS structure differential shot noise follows the reentrance peak observed in differential conductance, such that the differential Fano factor $(dS_{\mathrm{N}}/dV)/2eG\approx 2/3$ remains approximately constant (Fig. 3). Hence, the differential Fano factor is twice the normal value reflecting the fact that in an NS junction the current essentially results from the uncorrelated transfer of Cooper pairs. In Fig. 1 we note that at zero voltage, G_{NS} is 2% below G_{N}. This is due to a weak-localization effect resulting from the quantum interference between time-reversed paths of the electrons[11,14] yielding a different contribution to G_{NS} than to G_{N}.

If the N wire is only weakly connected to the superconductor, the differential conductance G probes the density of states of the superconductor. This is depicted in the upper inset of Fig. 4 where the conductance of a NIS structure is plotted as a function of voltage. However, at zero voltage, the coherent interplay between the Andreev-reflected and disorder-scattered electrons results in the reflectionless-tunneling effect increasing G_{NIS} and creating a peak around $V=0$ (Fig. 4). The reflectionless-tunneling effect may arise

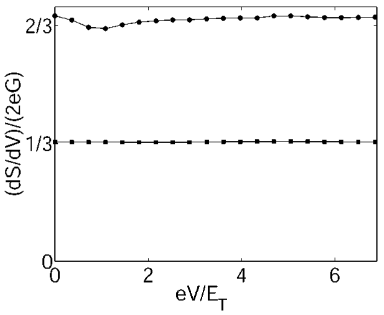

FIG. 3. Differential Fano factor $(dS/dV)/2eG$ as a function of voltage. The 95% confidence interval for the relative error is $\pm 1\%$. Circles, NS structure, squares, N structure. The small variation in the NS case is outside the error bars, but relatively smaller than the corresponding variations in G and dS/dV.

when there is a superconductor on the other side of the tunneling barrier and multiple scatterings by the tunneling barrier and by the disorder potential in the normal-metal area take place.[9–11]

As a test of our numerical results, we compare the obtained differential conductance G in the case of reflectionless tunneling to the expressions derived from the quasiclassical theory of nonequilibrium, inhomogeneous superconductivity[15,16] in the diffusive limit. To calculate the current for the present setup, we need to solve for the transverse distribution function (i.e., the symmetric part of the electron distribution function around the chemical potential of the superconductor) whose gradient determines the quasiparticle current. In the limit $r_b = R_B/R_{\mathrm{N}} \gg 1$, $eV \ll \Delta$, we obtain for G at $T=0$ (for details, see Ref. 16 and the references therein)

$$G = \frac{G_{\mathrm{N}}(\sin 2\sqrt{v} + \sinh 2\sqrt{v})}{4r_b^2\sqrt{v}(\cos^2\sqrt{v} + \sinh^2\sqrt{v}) + \sin 2\sqrt{v} + \sinh 2\sqrt{v}}, \tag{6}$$

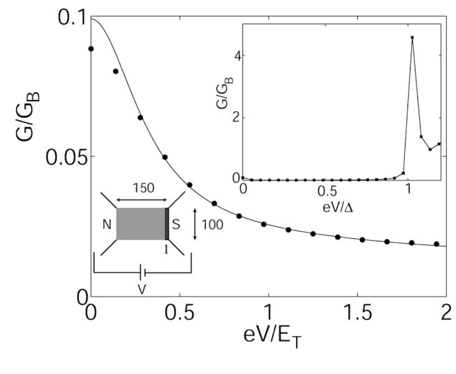

FIG. 4. Normalized differential conductance G/G_B as a function of voltage in the NIS structure depicted in the lower inset ($G_{\mathrm{N}}/G_B = 10$). Circles, scattering-matrix approach; solid line, quasiclassical theory (Ref. 13). Upper inset: differential conductance at the larger voltage scale. The 95% confidence interval for the relative error is $\pm 1\%$. The results in Figs. 4–6 were ensemble averaged over 300 realizations.

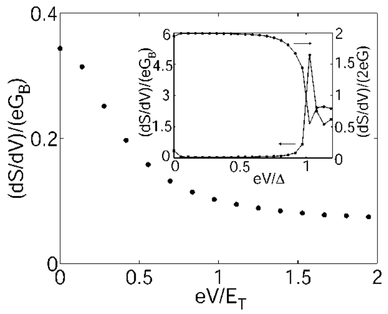

FIG. 5. Normalized differential shot noise $(dS/dV)/eG_B$ as a function of voltage. The 95% confidence interval for the relative error is $\pm 1\%$. Inset: Differential shot noise (squares) and differential Fano factor (circles) at the larger voltage scale.

where $v \equiv eV/E_T$ and G_{N} is the normal-state conductance of the diffusive wire. This is also plotted as a function of v in Fig. 4 and agrees well with the scattering-matrix approach.[13]

We have also calculated the differential shot noise as a function of voltage in the NIS structure (Fig. 5) using the scattering-matrix method. We observe that also the differential shot noise increases at zero voltage due to reflectionless tunneling. The inset in Fig. 5 illustrates the differential shot noise and the differential Fano factor at larger voltages. At voltages slightly above zero current and noise are suppressed since there are no single-particle states in the superconductor and the Andreev reflection probability is proportional to the square of the tunneling probability. At $V = \Delta/e$ the differential shot noise follows the conductance peak. The interplay between the Cooper-pair and single-electron transport is most clearly seen in the differential Fano factor. At voltages below Δ/e the Andreev reflection is the dominant charge transfer mechanism. Since the transmission probability through the barrier is small, at low voltages we obtain a Fano factor which is twice the Poissonian value. As voltage approaches Δ/e, the normal transmission probability increases and the system effectively behaves more like a normal conductor. Thus, the differential Fano factor quickly decreases to a value near unity. In the inset of Fig. 5 the Fano factor at $V=0$ is below the values obtained at somewhat higher voltages. This is due to the fact that the chosen value for $r_b = 10$ is not strictly in the tunneling limit.

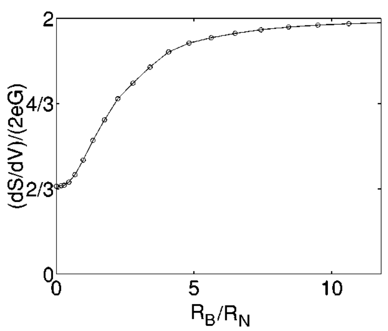

FIG. 6. Differential Fano factor $(dS/dV)/2eG$ in an NIS structure at $V=0$ as a function of resistance of the tunneling barrier R_B/R_{N} (measured in units of normal structure R_{N}). The 95% confidence interval for the relative error is $\pm 1\%$.

In order to illustrate the crossover from an ideal interface to the tunneling limit we have studied reflectionless tunneling by calculating the Fano factor as a function of the interface resistance R_B at zero voltage. The resistance R_N of the normal structure gives the characteristic scale for R_B, thus we plot the differential Fano factor as a function of R_B/R_N (Fig. 6). At large values of R_B, differential Fano factor approaches a limiting value two.

In conclusion, we have studied differential shot noise in normal-superconducting mesoscopic structures in the nonlinear regime at finite voltages. The superconducting proximity effect manifests itself as a well-known nonlinear reentrance behavior in the conductance at the voltages of the order of a few E_T/e. We have shown that also the shot noise exhibits a similar reentrance effect which keeps the differential Fano factor approximately constant as a function of the voltage. In the second part of the paper, we have considered a nonideal NS interface with an insulating barrier between the normal and superconducting regions. We find that also the differential shot noise exhibits a reflectionless-tunneling effect observed as an enhancement of the noise at zero voltage. Our calculations are consistent with the quasiclassical results and other previous work.

We acknowledge Ya. Blanter, J. C. Cuevas, F. Hekking, A. Kolek, and F. Wilhelm for discussions and comments. The numerical simulations have been performed at the Center for Scientific Computing (CSC, Finland). This work was supported by the Finnish Cultural Foundation and the Graduate School in Technical Physics at the Helsinki University of Technology.

[1] C. W. J. Beenakker and M. Büttiker, Phys. Rev. B **46**, 1889 (1992).
[2] C. W. J. Beenakker, Rev. Mod. Phys. **69**, 731 (1997).
[3] K. E. Nagaev, Phys. Lett. A **69**, 103 (1992).
[4] Ya. M. Blanter and M. Büttiker, Phys. Rep. **336**, 2 (2000).
[5] M. J. M. de Jong and C. W. J. Beenakker, Phys. Rev. B **49**, 16 070 (1994); B. A. Muzykantskii and D. E. Khmelnitskii, *ibid.* **50**, 3982 (1994).
[6] X. Jehl, M. Sanquer, R. Calemczuk, and D. Mailly, Nature (London) **405**, 50 (2000).
[7] F. Taddei and R. Fazio, Phys. Rev. B **65**, 134 522 (2002).
[8] W. Belzig and Yu. V. Nazarov, Phys. Rev. Lett. **87**, 067006 (2001).
[9] B. J. van Wees, P. de Vries, P. Magnee, and T. M. Klapwijk, Phys. Rev. Lett. **69**, 510 (1992).
[10] A. Kastalsky, A. W. Kleinsasser, L. H. Greene, R. Bhat, F. P. Milliken, and J. P. Harbison, Phys. Rev. Lett. **67**, 3026 (1991).
[11] I. K. Marmorkos, C. W. J. Beenakker, and R. A. Jalabert, Phys. Rev. B **48**, 2811 (1993).
[12] T. T. Heikkilä, M. M. Salomaa, and C. J. Lambert, Phys. Rev. B **60**, 9291 (1999).
[13] To obtain an agreement with the two approaches, we had to rescale the Thouless energy in Eq. (6) by a numerical factor of order 3.8.
[14] Y. V. Nazarov, Phys. Rev. B **52**, 4720 (1995).
[15] W. Belzig, F. K. Wilhelm, G. Schön, C. Bruder, and A. D. Zaikin, Superlattices Microstruct. **25**, 1251 (1999).
[16] C. J. Lambert and R. Raimondi, J. Phys.: Condens. Matter **10**, 901 (1998).